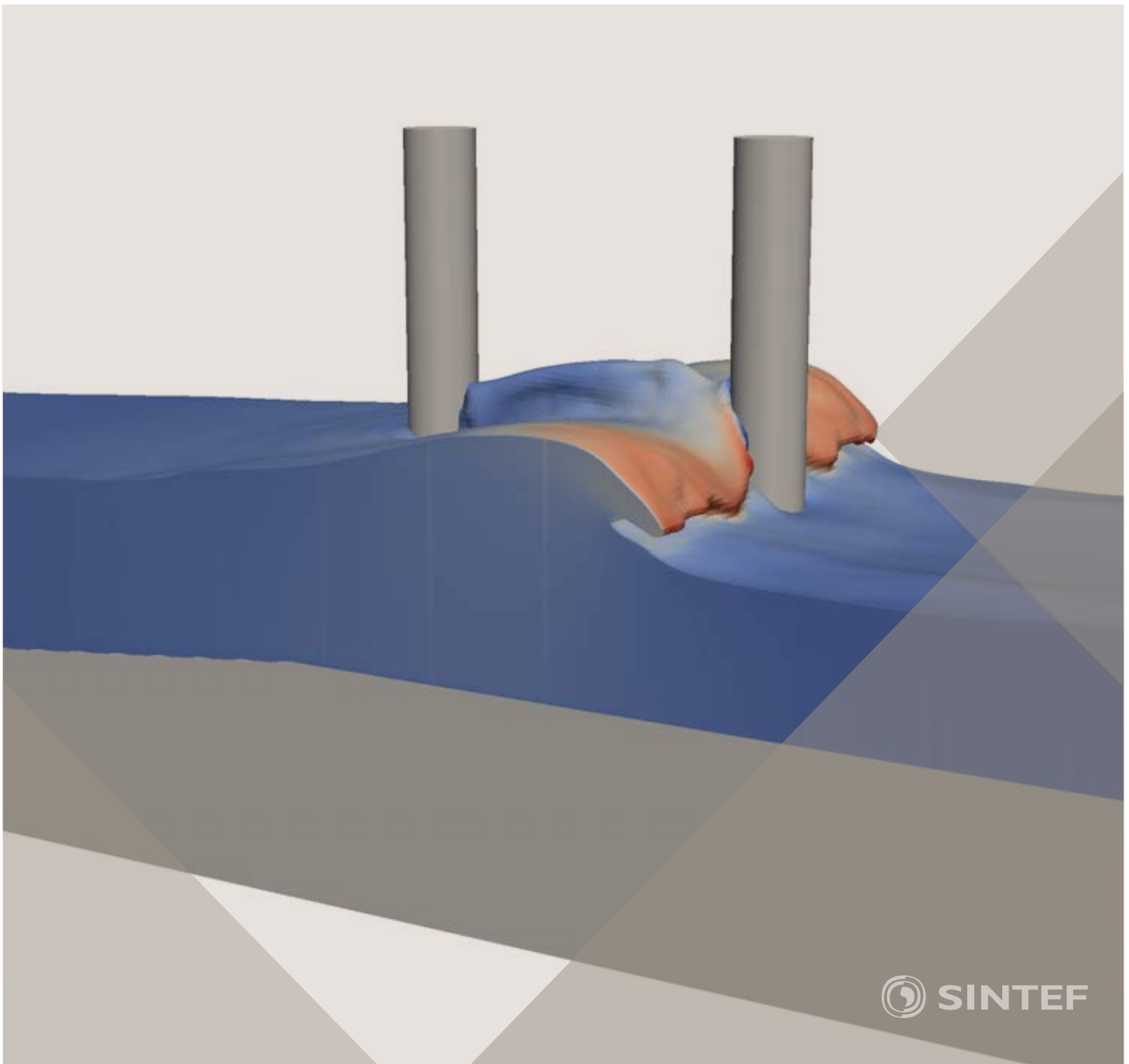


Proceedings of the 12th International Conference on
Computational Fluid Dynamics in the Oil & Gas,
Metallurgical and Process Industries

Progress in Applied CFD – CFD2017



SINTEF Proceedings

Editors:

Jan Erik Olsen and Stein Tore Johansen

Progress in Applied CFD – CFD2017

Proceedings of the 12th International Conference on Computational Fluid Dynamics
in the Oil & Gas, Metallurgical and Process Industries

SINTEF Academic Press

SINTEF Proceedings no 2

Editors: Jan Erik Olsen and Stein Tore Johansen

Progress in Applied CFD – CFD2017

Selected papers from 10th International Conference on Computational Fluid Dynamics in the Oil & Gas, Metallurgical and Process Industries

Key words:

CFD, Flow, Modelling

Cover, illustration: Arun Kamath

ISSN 2387-4295 (online)

ISBN 978-82-536-1544-8 (pdf)

© Copyright SINTEF Academic Press 2017

The material in this publication is covered by the provisions of the Norwegian Copyright Act. Without any special agreement with SINTEF Academic Press, any copying and making available of the material is only allowed to the extent that this is permitted by law or allowed through an agreement with Kopinor, the Reproduction Rights Organisation for Norway. Any use contrary to legislation or an agreement may lead to a liability for damages and confiscation, and may be punished by fines or imprisonment

SINTEF Academic Press

Address: Forskningsveien 3 B
 PO Box 124 Blindern
 N-0314 OSLO

Tel: +47 73 59 30 00

Fax: +47 22 96 55 08

www.sintef.no/byggforsk

www.sintefbok.no

SINTEF Proceedings

SINTEF Proceedings is a serial publication for peer-reviewed conference proceedings on a variety of scientific topics.

The processes of peer-reviewing of papers published in SINTEF Proceedings are administered by the conference organizers and proceedings editors. Detailed procedures will vary according to custom and practice in each scientific community.

PREFACE

This book contains all manuscripts approved by the reviewers and the organizing committee of the 12th International Conference on Computational Fluid Dynamics in the Oil & Gas, Metallurgical and Process Industries. The conference was hosted by SINTEF in Trondheim in May/June 2017 and is also known as CFD2017 for short. The conference series was initiated by CSIRO and Phil Schwarz in 1997. So far the conference has been alternating between CSIRO in Melbourne and SINTEF in Trondheim. The conferences focuses on the application of CFD in the oil and gas industries, metal production, mineral processing, power generation, chemicals and other process industries. In addition pragmatic modelling concepts and bio-mechanical applications have become an important part of the conference. The papers in this book demonstrate the current progress in applied CFD.

The conference papers undergo a review process involving two experts. Only papers accepted by the reviewers are included in the proceedings. 108 contributions were presented at the conference together with six keynote presentations. A majority of these contributions are presented by their manuscript in this collection (a few were granted to present without an accompanying manuscript).

The organizing committee would like to thank everyone who has helped with review of manuscripts, all those who helped to promote the conference and all authors who have submitted scientific contributions. We are also grateful for the support from the conference sponsors: ANSYS, SFI Metal Production and NanoSim.

Stein Tore Johansen & Jan Erik Olsen



Organizing committee:

Conference chairman: Prof. Stein Tore Johansen

Conference coordinator: Dr. Jan Erik Olsen

Dr. Bernhard Müller

Dr. Sigrid Karstad Dahl

Dr. Shahriar Amini

Dr. Ernst Meese

Dr. Josip Zoric

Dr. Jannike Solsvik

Dr. Peter Witt

Scientific committee:

Stein Tore Johansen, SINTEF/NTNU

Bernhard Müller, NTNU

Phil Schwarz, CSIRO

Akio Tomiyama, Kobe University

Hans Kuipers, Eindhoven University of Technology

Jinghai Li, Chinese Academy of Science

Markus Braun, Ansys

Simon Lo, CD-adapco

Patrick Segers, Universiteit Gent

Jiyuan Tu, RMIT

Jos Derksen, University of Aberdeen

Dmitry Eskin, Schlumberger-Doll Research

Pär Jönsson, KTH

Stefan Pirker, Johannes Kepler University

Josip Zoric, SINTEF

CONTENTS

PRAGMATIC MODELLING	9
On pragmatism in industrial modeling. Part III: Application to operational drilling	11
CFD modeling of dynamic emulsion stability	23
Modelling of interaction between turbines and terrain wakes using pragmatic approach	29
FLUIDIZED BED	37
Simulation of chemical looping combustion process in a double looping fluidized bed reactor with cu-based oxygen carriers.....	39
Extremely fast simulations of heat transfer in fluidized beds.....	47
Mass transfer phenomena in fluidized beds with horizontally immersed membranes	53
A Two-Fluid model study of hydrogen production via water gas shift in fluidized bed membrane reactors	63
Effect of lift force on dense gas-fluidized beds of non-spherical particles	71
Experimental and numerical investigation of a bubbling dense gas-solid fluidized bed	81
Direct numerical simulation of the effective drag in gas-liquid-solid systems	89
A Lagrangian-Eulerian hybrid model for the simulation of direct reduction of iron ore in fluidized beds.....	97
High temperature fluidization - influence of inter-particle forces on fluidization behavior	107
Verification of filtered two fluid models for reactive gas-solid flows	115
BIOMECHANICS.....	123
A computational framework involving CFD and data mining tools for analyzing disease in carotid artery	125
Investigating the numerical parameter space for a stenosed patient-specific internal carotid artery model.....	133
Velocity profiles in a 2D model of the left ventricular outflow tract, pathological case study using PIV and CFD modeling.....	139
Oscillatory flow and mass transport in a coronary artery.....	147
Patient specific numerical simulation of flow in the human upper airways for assessing the effect of nasal surgery.....	153
CFD simulations of turbulent flow in the human upper airways	163
OIL & GAS APPLICATIONS	169
Estimation of flow rates and parameters in two-phase stratified and slug flow by an ensemble Kalman filter	171
Direct numerical simulation of proppant transport in a narrow channel for hydraulic fracturing application	179
Multiphase direct numerical simulations (DNS) of oil-water flows through homogeneous porous rocks	185
CFD erosion modelling of blind tees	191
Shape factors inclusion in a one-dimensional, transient two-fluid model for stratified and slug flow simulations in pipes	201
Gas-liquid two-phase flow behavior in terrain-inclined pipelines for wet natural gas transportation	207

NUMERICS, METHODS & CODE DEVELOPMENT	213
Innovative computing for industrially-relevant multiphase flows	215
Development of GPU parallel multiphase flow solver for turbulent slurry flows in cyclone.....	223
Immersed boundary method for the compressible Navier–Stokes equations using high order summation-by-parts difference operators	233
Direct numerical simulation of coupled heat and mass transfer in fluid-solid systems	243
A simulation concept for generic simulation of multi-material flow, using staggered Cartesian grids.....	253
A cartesian cut-cell method, based on formal volume averaging of mass, momentum equations.....	265
SOFT: a framework for semantic interoperability of scientific software	273
POPULATION BALANCE	279
Combined multifluid-population balance method for polydisperse multiphase flows	281
A multifluid-PBE model for a slurry bubble column with bubble size dependent velocity, weight fractions and temperature.....	285
CFD simulation of the droplet size distribution of liquid-liquid emulsions in stirred tank reactors	295
Towards a CFD model for boiling flows: validation of QMOM predictions with TOPFLOW experiments	301
Numerical simulations of turbulent liquid-liquid dispersions with quadrature-based moment methods.....	309
Simulation of dispersion of immiscible fluids in a turbulent couette flow	317
Simulation of gas-liquid flows in separators - a Lagrangian approach.....	325
CFD modelling to predict mass transfer in pulsed sieve plate extraction columns	335
BREAKUP & COALESCENCE	343
Experimental and numerical study on single droplet breakage in turbulent flow	345
Improved collision modelling for liquid metal droplets in a copper slag cleaning process	355
Modelling of bubble dynamics in slag during its hot stage engineering.....	365
Controlled coalescence with local front reconstruction method	373
BUBBLY FLOWS	381
Modelling of fluid dynamics, mass transfer and chemical reaction in bubbly flows	383
Stochastic DSMC model for large scale dense bubbly flows.....	391
On the surfacing mechanism of bubble plumes from subsea gas release.....	399
Bubble generated turbulence in two fluid simulation of bubbly flow	405
HEAT TRANSFER	413
CFD-simulation of boiling in a heated pipe including flow pattern transitions using a multi-field concept	415
The pear-shaped fate of an ice melting front	423
Flow dynamics studies for flexible operation of continuous casters (flow flex cc).....	431
An Euler-Euler model for gas-liquid flows in a coil wound heat exchanger.....	441
NON-NEWTONIAN FLOWS.....	449
Viscoelastic flow simulations in disordered porous media	451
Tire rubber extrudate swell simulation and verification with experiments	459
Front-tracking simulations of bubbles rising in non-Newtonian fluids.....	469
A 2D sediment bed morphodynamics model for turbulent, non-Newtonian, particle-loaded flows.....	479

METALLURGICAL APPLICATIONS.....	491
Experimental modelling of metallurgical processes	493
State of the art: macroscopic modelling approaches for the description of multiphysics phenomena within the electroslag remelting process	499
LES-VOF simulation of turbulent interfacial flow in the continuous casting mold	507
CFD-DEM modelling of blast furnace tapping	515
Multiphase flow modelling of furnace tapholes	521
Numerical predictions of the shape and size of the raceway zone in a blast furnace.....	531
Modelling and measurements in the aluminium industry - Where are the obstacles?	541
Modelling of chemical reactions in metallurgical processes.....	549
Using CFD analysis to optimise top submerged lance furnace geometries	555
Numerical analysis of the temperature distribution in a martensitic stainless steel strip during hardening.....	565
Validation of a rapid slag viscosity measurement by CFD.....	575
Solidification modeling with user defined function in ANSYS Fluent.....	583
Cleaning of polycyclic aromatic hydrocarbons (PAH) obtained from ferroalloys plant.....	587
Granular flow described by fictitious fluids: a suitable methodology for process simulations	593
A multiscale numerical approach of the dripping slag in the coke bed zone of a pilot scale Si-Mn furnace.....	599
INDUSTRIAL APPLICATIONS	605
Use of CFD as a design tool for a phosphoric acid plant cooling pond	607
Numerical evaluation of co-firing solid recovered fuel with petroleum coke in a cement rotary kiln: Influence of fuel moisture	613
Experimental and CFD investigation of fractal distributor on a novel plate and frame ion-exchanger	621
COMBUSTION	631
CFD modeling of a commercial-size circle-draft biomass gasifier.....	633
Numerical study of coal particle gasification up to Reynolds numbers of 1000.....	641
Modelling combustion of pulverized coal and alternative carbon materials in the blast furnace raceway	647
Combustion chamber scaling for energy recovery from furnace process gas: waste to value	657
PACKED BED.....	665
Comparison of particle-resolved direct numerical simulation and 1D modelling of catalytic reactions in a packed bed	667
Numerical investigation of particle types influence on packed bed adsorber behaviour	675
CFD based study of dense medium drum separation processes	683
A multi-domain 1D particle-reactor model for packed bed reactor applications.....	689
SPECIES TRANSPORT & INTERFACES	699
Modelling and numerical simulation of surface active species transport - reaction in welding processes	701
Multiscale approach to fully resolved boundary layers using adaptive grids.....	709
Implementation, demonstration and validation of a user-defined wall function for direct precipitation fouling in Ansys Fluent.....	717

FREE SURFACE FLOW & WAVES	727
Unresolved CFD-DEM in environmental engineering: submarine slope stability and other applications.....	729
Influence of the upstream cylinder and wave breaking point on the breaking wave forces on the downstream cylinder	735
Recent developments for the computation of the necessary submergence of pump intakes with free surfaces	743
Parallel multiphase flow software for solving the Navier-Stokes equations	752
PARTICLE METHODS	759
A numerical approach to model aggregate restructuring in shear flow using DEM in Lattice-Boltzmann simulations	761
Adaptive coarse-graining for large-scale DEM simulations.....	773
Novel efficient hybrid-DEM collision integration scheme.....	779
Implementing the kinetic theory of granular flows into the Lagrangian dense discrete phase model.....	785
Importance of the different fluid forces on particle dispersion in fluid phase resonance mixers	791
Large scale modelling of bubble formation and growth in a supersaturated liquid.....	798
FUNDAMENTAL FLUID DYNAMICS	807
Flow past a yawed cylinder of finite length using a fictitious domain method	809
A numerical evaluation of the effect of the electro-magnetic force on bubble flow in aluminium smelting process.....	819
A DNS study of droplet spreading and penetration on a porous medium.....	825
From linear to nonlinear: Transient growth in confined magnetohydrodynamic flows.....	831

USE OF CFD AS A DESIGN TOOL FOR A PHOSPHORIC ACID PLANT COOLING POND

Aurélien DAVAILLES^{1*} , Sylvain DEVYNCK¹

TechnipFMC - Paris Operating Center, Paris la Défense, FRANCE

* Corresponding author, E-mail: aurelien.davailles@technipfmc.com

ABSTRACT

Phosphate fertilizer plants are installations constantly evolving which make their design a challenging task. Phosphogypsum, a by-product of the manufacture of phosphoric acid, is piled up, forming stacks which may eventually alter the process efficiency as they encroach on process cooling ponds and locally modify the airflow fields. The easier access to high performance computing and the improvement of software capabilities allow to fully consider today the use of CFD within tight-schedule industrial projects, even the ones involving large-size geometry. As an example we describe how CFD can be efficiently used as a design tool for the revamping of a phosphate fertilizer complex. The use of recently emerged multi-software optimization tool is also explored as a way to enhance the engineering time dedicated to this problem.

Keywords: CFD, Fluid-Fluid interaction, Heat exchange, Optimization, Pollutant dispersion.

NOMENCLATURE

Greek Symbols

α Water mass fraction.

Latin Symbols

V Velocity, [m/s].

T Temperature [°C].

z_0 Roughness length, [m].

Sub/superscripts

a Air.

p Pond

INTRODUCTION

The enhanced accessibility to faster cores has led to an important evolution of high computing performance (HPC) for CFD. In addition, most of the current commercial softwares are now well optimized to take advantage of this available higher power resources, allowing large-size geometry parallelization. This has opened up new opportunities for CFD to be part of industrial projects as a design tool in domains where it was not a conceivable option just a few years ago, due to the incompatibility between the project schedules and the

time consuming calculations. Furthermore, CFD studies on the atmospheric boundary layer are now common [DUYNKERKE, 1988] [VENDEL et al, 2010] and allow to model a complete plant subjected to various weather conditions. Based on Pasquill classes [PASQUILL, 1971], different wind velocity, temperature and turbulence profiles can be applied to represent real atmospheric conditions. In Oil & Gas industry, two frequent examples are the Hot Air Recirculation studies performed on Liquefied Natural Gas (LNG) trains and the pollutant dispersion studies around onshore and/or offshore installations [DEVYNCK, 2016]. Another less familiar application involving the modeling of large geometry and for which CFD can be a helpful design option is the phosphate fertilizer plant.

This kind of plant may be associated with several problematics such as fluoride dispersion, steam fog formation or process thermal management. Fluoride is a major pollutant involved in the phosphoric acid production process which usually consists of the reaction between phosphate rock and sulphuric acid (wet process). Its release in the atmosphere from the evaporative cooling pond surface must be carefully monitored to ensure the respect of the regulations. Moreover, the cooling process taking place in the ponds leads to an important increase of the water content in the ambient air, which can cause steam fog formation under unfavourable weather conditions. Whether it is for the dispersion of fluoride or the steam fog formation prediction, not only CFD can allow to assess the situation but also to explore improvement solutions.

Another concern regarding the phosphate fertilizer plants comes from the formation over time of large phosphogypsum stacks which may eventually lead to the necessity to revamp the plant. The phosphogypsum, a by-product of the manufacture of the phosphoric acid during the so called wet process, is mixed with water to form a slurry, then continuously piled up in settling ponds which will turn into massive gypsum stacks after years of service. About 5 tons of phosphogypsum are produced for each ton of phosphoric acid [GOWARIKER et al, 2009]. To allow the gypsum stack expansion, new deposit areas must be defined. The conversion of a cooling pond into a settling pond is then a possible solution even though it leads to the reduction of the heat

exchange surface. As a result, new ways to exchange energy or to reduce the process total heat duty requirement must be found. The easiest way to achieve this may be by revamping the process in order to reduce the total dissipated energy and to optimize the remaining exchange surface. Revamping plants is a quite common task for Oil & Gas engineering companies nowadays and CFD can be used to support the optimization of the remaining pond surface.

MODEL DESCRIPTION

Overall geometry

To account for a phosphate site production, a typical area has been reproduced. It consists in two gypsum stacks whose only one is still active with a settling pond at the top. Three cooling ponds are used on that plant, including one at the top of the non-active gypstack. Surrounding elements such as process units and houses of the residential area have also been modeled (Figure 1). The atmospheric part of the domain is modeled by a box whose dimensions are 2km x 2.5km x 1km.

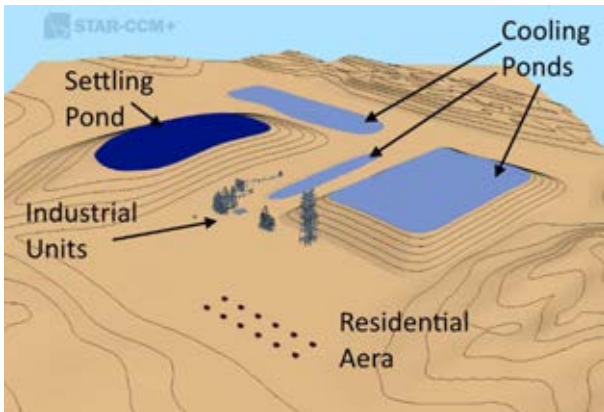


Figure 1: Overall domain

The presence of irregular terrain close to the site can be included into the simulation starting either from 2D elevation lines or directly from a 3D topography surface. Using STAR-CCM+ surface wrapper we reconstructed a CFD compatible ground surface.

In the following demonstration study, the irregular terrain elevation has been imported as STL files while stacks have been entirely built from the 3D-CAD modeler of STAR-CCM+. All parts of interest for the study must be included in the computational domain in order to take into account the congestion and the air flow disturbance. Moreover, this could also be of importance for controlling precisely the amount of pollutant in the installation area.

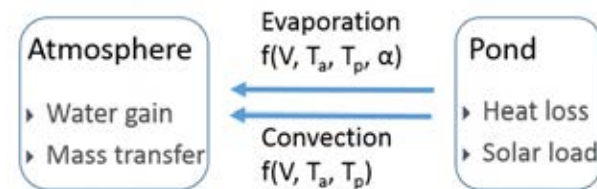
A residential area represented by 12 houses has been implemented at about 500 meters of the closest pond. Likewise, process industrial structures are positioned at about 100 m from the pond.

Fluid-Fluid interaction

To account for the evaporation taking place from the pond surface without computing the real gas-liquid

interface, we modeled it as a fluid-structure interface. Two independent fluid regions are exchanging data through the interface in order to compute the calibrated heat and mass exchange. Several benefits come from the separation of the two regions: the physics is simplified as there is no more need for multiphase flow modeling. Instead, two single phase flow calculations are performed simultaneously and only an exchange of some specific values at the interface is required. Using data mapping technique with nearest neighbour interpolation, water temperature value is sent to the atmosphere region whereas the calculated evaporative and convective heat fluxes values are transmitted to the pond region to cool down the liquid.

Several field functions accounting for the evaporative and convective heat fluxes and the water mass flow rate at the air/pond interface have been defined. The main local parameters used by the solver to feed those functions are the air velocity, the air temperature, the relative humidity and the water temperature. The different exchanges taking place between the two fluid domains are summarized by the following diagram.



The evaporation correlation is based on daily experimental data measurements over several years and is detailed in § Heat management computations.

Another important advantage arising from the flat interface hypothesis is to allow the use of coarser meshes. Table 1 gives a comparison of the mesh size of two identical domains varying only by the modeling approach (1 fluid region versus 2 fluid regions).

Table 1: Number of cells

	Air	Water	TOTAL
2 regions	184,858	102,090	286,948
1 region	2,240,000	717,066	2,957,142

It is obvious that adopting the two separated fluid zone modeling will allow a significant computational time reduction which is preferable for the purpose of conducting optimization study which can require to perform numerous simulation runs.

Mesh

Due to the large surface and the very small depth of the ponds, the thin mesher technique has been used in the water region. Ten cells have been generated over the water depth to discretise sufficiently the cooling pond. There is no need to use a conformal mesh at the interface due to the employed interpolation technique (§ Fluid-Fluid Interaction). Thus, with a cell size of the same magnitude at both interface sides, yet adopting two

different meshing method for the fluid zones, the final mesh can be coarser while remaining relevant to model the heat exchange and the flow in the two regions. In the air zone, a trimmed mesh has been used with one prism layer generated on the ground. The ground surface cell size has been set to 5m while a 2m size has been imposed on the pond surface. During the surface wrapping operation, different target sizes have been defined on the structure elements according to the desired level of precision. The minimum cell size allowable has been set to 10 % of the base size.

The Figure 2 shows the differences between the initial faceted surface (STL) and two generated surface meshes set with different base sizes, respectively 5 m and 10 m.

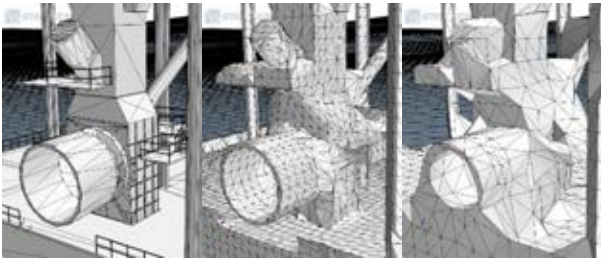


Figure 2: STL file, Wrap 5m, Wrap 10m

Given the potential for the rapid growth of the total cell number, only the areas of interest, such as the air intakes or the areas nearby the workers should be precisely discretised.

Pond Optimization

Following the removal of one of the cooling pond to allow space for the active gypsum stack expansion, a significant surface which was dedicated to the dissipation of the energy is no longer available. Consequently, modifications must be made to the process to recover the lost heat duty, thus ensuring to maintain the process efficiency. In order to achieve this objective, the remaining cooling ponds must be optimized as well to make them the most efficient possible.

On this basis, the second pond which offers the highest potential due to its larger size, has been modeled separately with the purpose to optimize the surface heat exchange. As the overall geometry of the pond cannot be modified, only realistic on-site implementations have been explored such as modification of the water inlets/outlets position and the addition of elements to modify the water distribution, such as dikes.

Figure 3 highlights the CFD study domain which includes only the cooling pond and the non-active gypsum stack to keep the number of cells to a reasonable amount. Indeed, the optimization study can require a lot of calculation runs to determine the global optimum or to plot a Pareto front which helps to determine the feasible designs depending on the defined constraints and objectives.

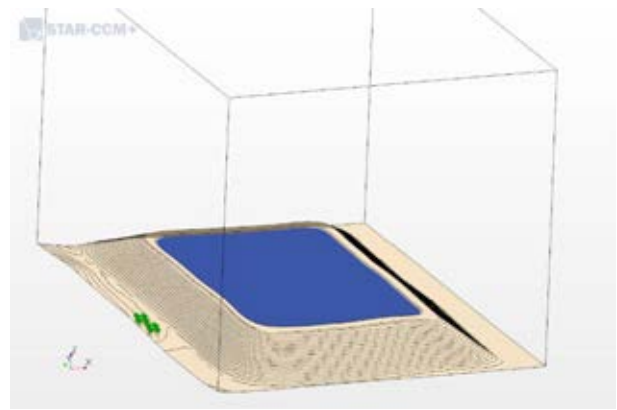


Figure 3: Optimization domain

The optimization tool used for this study is HEEDS which is a multidisciplinary design exploration software from Siemens PLM Software. After the definition of several parameters adjustable by the solver and several target objectives, the selected optimization algorithm will explore the whole space design in order to find local or global optimum. As this exploration process is automated within HEEDS, the final geometry and mesh model must be robust to ensure the good convergence of the different calculations. Consequently, all the standard manual manipulations such as “surface repair” or “diagnostics” are avoided and must be configured to be automatically performed.

In order to modify the water distribution inside the pond, dikes have been created via the 3D-CAD modeler to be added to the pond model. The parameters defined as being modifiable by the software to find the better designs are:

- Number of dikes (from 1 to 10).
- Depth of the pond (from 0.5m to 5m)
- Orientation of the dikes (North-South or East-West)
- Aperture between side of the pond and dikes (20 to 200m)

A JAVA macro is also executed before the start of the simulation in order to modify the position of the water inlet inside the pond. Indeed, depending on the number of dikes and their orientation, the inlet may be located at three different locations, while the outlet remains fixed.

As a finer mesh is required close to the dikes, the total number of cells in the domain will change significantly according to the parameter set configuration. The total number of cells can vary between 300,000 cells and 2,500,000 cells.

Two objectives have been defined: improve the surface heat transfer and reduce the investment costs (CAPEX). On a practical level, this involves the lowest outlet temperature possible while minimizing the dikes length.

Boundary and Operating conditions

Air domain

The atmospheric domain has been set to orient the cell faces perpendicularly to the wind direction. Wind is coming from the east direction with a neutral wind stability profile (Pasquill class D). Wind velocity is 3 m/s at 10 m elevation. The wind temperature is assumed to be constant and equal to 25°C.

The two side faces parallel to the wind direction are considered as symmetry planes, such as the top of the atmospheric box. The last bounding box face has been set as a pressure outlet.

The atmospheric boundary layer has been modeled through the best practices of STAR-CCM+ and the roughness of the ground has been set to represent an agricultural land with some large obstacles by a distance of 500 meters ($z_0=0.035$).

On the water surface, a slip condition for air has been set. That leads to increase the wind velocity far from the side of the pond. A water mass flux source term has been defined. It depends on the wind velocity, the air temperature, the water content and the water temperature (see § Fluid-Fluid Interaction). Convective and evaporative heat transfer are computed via the correlations explained above. A realizable k-epsilon turbulence model has been used.

Water domain

The pond's bottom and side faces are considered adiabatic with a no-slip condition. The interface is treated like a free surface, i.e with a slip condition and with a thermal heat sink corresponding to the evaporation and the convection heat flux. A realizable k-epsilon turbulence model has been used.

RESULTS

Pollutant dispersion

Fluoride emissions from the ponds may raise concerns if the concentration reaches the regulatory limits. Safety and environmental studies are a large part of all the industrial projects. They aim to ensure the protection of the site workers and the population living in the plant vicinity. It is for this reason that the fluoride released by the eastern stack surface has been studied using a multi-gas approach.

The Figure 4 represents an overhead view of the plant and highlights the fluoride plume expansion. The wind coming from the right face of the atmospheric box (south east direction) drives the pollutant towards the installations and the residential area.

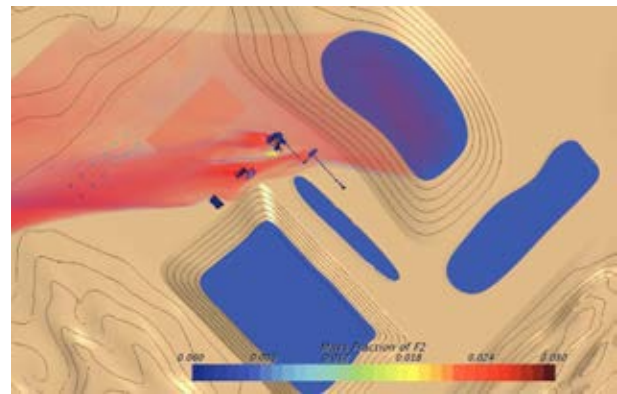


Figure 4: Fluorine plume expansion

The concentration of fluoride can also be displayed on the wall of the area of interest such as the residential area or the process equipment. Due to the discrepancy between the regulatory limits regarding the working area and the residential area (8 hour exposures vs yearly exposure) two scales of concentration must be plotted. On that example, an 8-hour mass fraction exposure limit of 0.027 (fictional value) of fluoride is drawn in Figure 5 on working area and a yearly mass fraction exposure limit of 0.015 (fictional value) of fluoride on the houses representing the residential area on Figure 6.

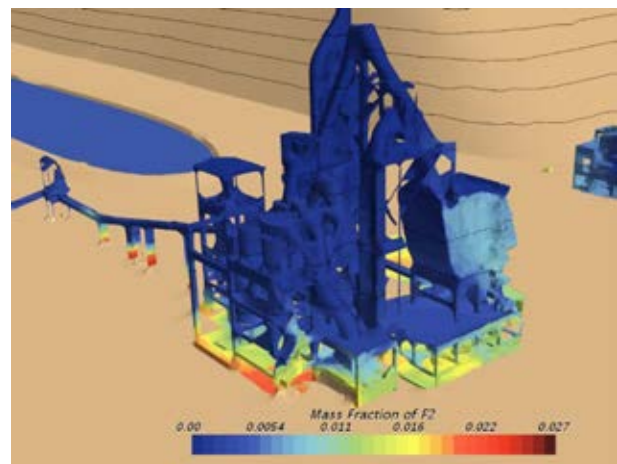


Figure 5: 8Hr exposure limit on working area

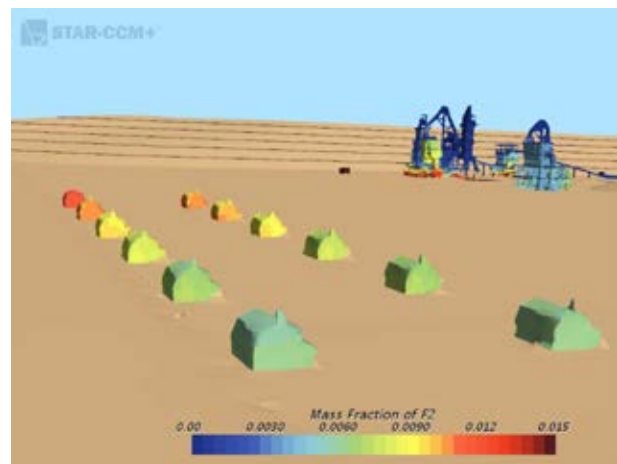


Figure 6: 1yr exposure limit on residential area

Heat management computations

The main role of the cooling ponds is to exchange a large amount of heat with the atmosphere, thus reducing the process water temperature. Any modification of the upstream process (inlet water temperature, water flowrate, etc) or of the cooling pond surface will affect its performances.

Base case

First of all, the active configuration has been modeled and compared to experimental on-site measurements. Three ponds are used to cool the process water, two on the ground level and one at the top of an old gypsum stack.

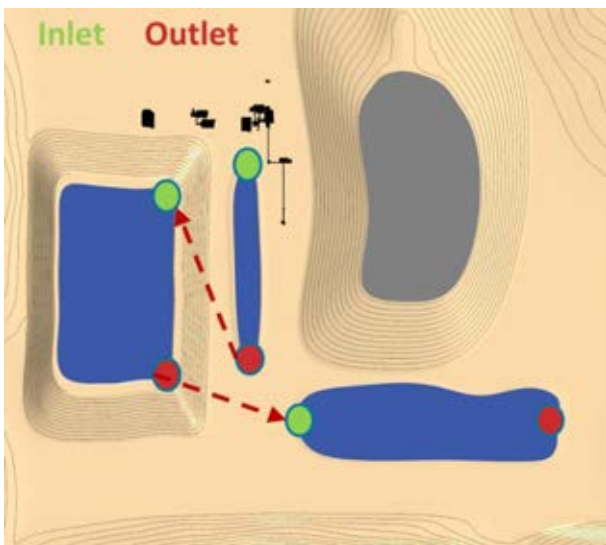


Figure 7: Base case modeling

According to on-site daily measurements, an evaporation correlation has been established depending on wind velocity, air temperature, water content in air (moisture) and water temperature. The way to exchange the values between the water and the air is described in § Fluid-Fluid Interaction. The convective heat transfer has also been taken into account depending on wind velocity, air temperature and water temperature.

Figure 7 represents the running order of the three ponds. The water is entering in the first and smaller pond at 48°C. Figure 8 shows the computed water surface temperature in the different ponds.

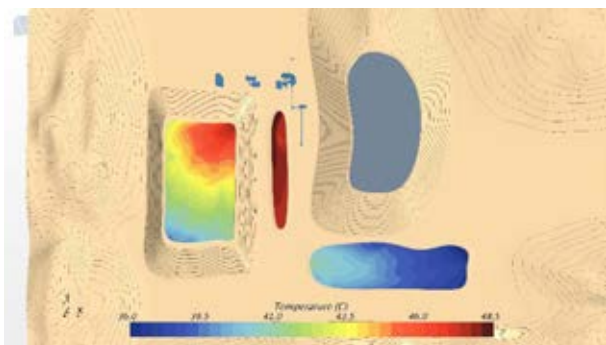


Figure 8: Base case surface temperature

The calculation allowed to highlight the contribution of the last – and soon to be remove - pond to the total heat exchange. Water temperature drops by 4°C in this pond which represents 52 MW (about 30% of total heat exchange).

Pond optimization

All the results extracted from STARCCM+ by HEEDS have been compared to a base case without dikes and a pond depth of 2m (Figure 9). The outlet temperature is 44.43°C and the error margin has been estimated to be 0.2°C (5% of the heat exchange). More than 120 computations have been performed, including less than 15% that have failed due to divergence problems or results inconsistency.

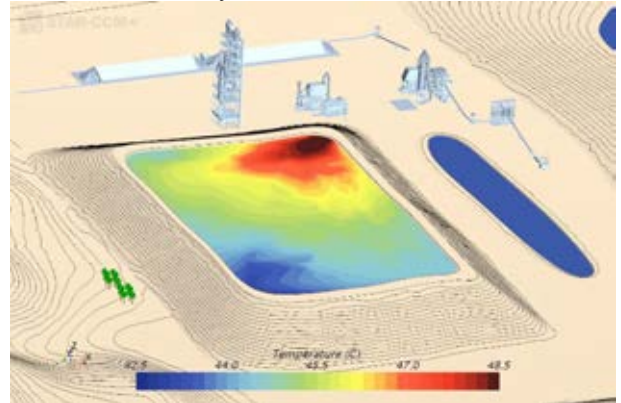


Figure 9: Optimization - No dikes, 2m depth

Some of the optimization results were very close to each other, within the error margin. That led to select not one, but several “best design” and to extract the trends regarding the effects of the different parameters.

As an example, we present two different solution designs leading to an equivalent outlet temperature (Figure 10 and Figure 11):

- 6 horizontal dikes, large opening, small depth
Outlet temperature = 43.8°C
Heat duty gain = 15.2%

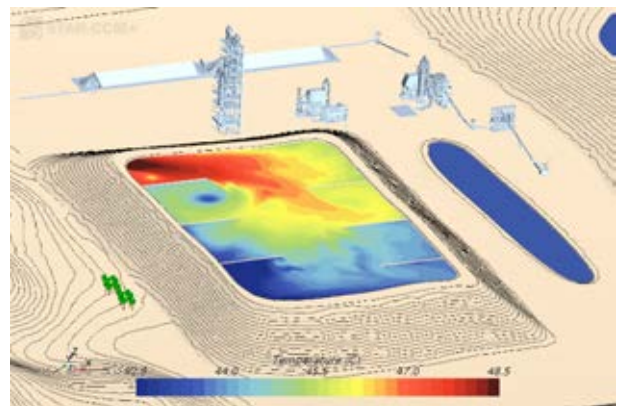


Figure 10: 6 horiz. dikes, large opening, small depth

- 1 horizontal dike, large opening, small depth
Outlet temperature = 43.65°C
Heat duty gain = 19%

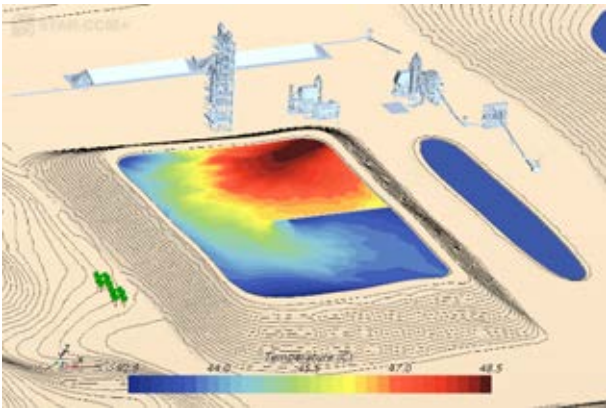


Figure 11: 1 horiz. dike, large opening, small depth

Figure 12 describes an analysis chart coming from HEEDS which allows to quickly identify trends by understanding the connections between the different design parameters. In our case it allowed to identify the following trends:

- Both horizontal and vertical dike positioning are possible
- The number of dikes may change from 1 to 7 in the best designs
- The aperture at the end of the dikes may be large or medium, depending on the number of dikes
- Depth seems to be the most influencing parameter and should be kept to a low value to improve the results.

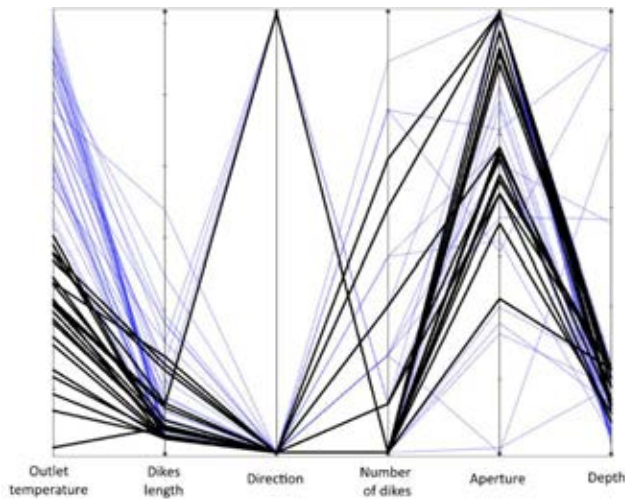


Figure 12: Connections between design parameters

CONCLUSION

Through the example of the revamping of a phosphate fertilizer plant, we have demonstrated that using CFD as

a design exploration tool for large installations is no longer a pipe dream. Even without a proper 3D-CAD model to start from, different strategies to reconstruct the model into the CFD software are possible, such as using the surface wrapper tool. Although the use of this wrapping technique makes more difficult the calibration and automation of the exchanges between the CFD and Design exploration softwares, it is something achievable.

In the case we have studied, a first CFD model of the active plant configuration has been developed and the simulations that followed have allowed to quantify the heat duty provided by each of the plant cooling ponds. In order to find solutions to recover the lost duty, the multidisciplinary design exploration software HEEDS has been used to drive numerous CFD simulation runs. These calculations did not allow to establish a typical Pareto front as the defined two objectives weren't incompatible with each other. No parameters among the ones we allowed the software to explore turned out to be a real game changer by itself regarding the pond efficiency. However, a list of best designs has been determined quickly thanks to the software, allowing to increase the pond efficiency of about 20%.

While we are just starting to explore the use of design exploration software to drive our CFD simulations, this test case has shown us very promising results regarding the quantity of valuable information that can be extracted in a very short time using this approach.

REFERENCES

- DEVYNCK, S., (2016) "Using Computational Fluid Dynamics to increase profitability", *In.Brief, GPA*, 09-2016
- DUYNKERKE, P. G. (1988). "Application of the E-ε turbulence closure model to the neutral and stable atmospheric boundary layer", *Journal of the atmospheric sciences*, 45(5), 865-880.
- GOWARIKER, V, et al. "The fertilizer encyclopedia." *John Wiley & Sons, 2009.*
- PASQUILL, F. "Wind structure in the atmospheric boundary layer." *Philosophical Transactions of the Royal Society of London A: Mathematical, Physical and Engineering Sciences*, 1971, vol. 269, no 1199, p. 439-456.
- VENDEL, F., et al. (2010). "Modelling diabatic atmospheric boundary layer using a RANS CFD code with k-epsilon turbulence closure". *13th Conference on Harmonisation within Atmospheric Dispersion Modelling for Regulatory Purposes.*